Palestine Journal of Mathematics

Vol 13(Special Issue I)(2024) , 66–78

ADAPTIVE FINITE VOLUME SCHEME FOR AIR QUALITY ON VERTEX-CENTERED MESH

Abdelaziz Chahed, Amal Bergam, Anouar El Harrak and Hatim Tayeq

MSC 2010 Classifications: Primary 35Q35; Secondary 65M08, 65M12, 76M12, 76R50, 92E20.

Keywords and phrases: Finite-volume method, Vertex-centered, Advection-Diffusion-Reaction Equation, Dominant Advection, Advective Scheme, Air Quality.

Abstract We propose in this paper a vertex-centered finite volume scheme that can efficiently handle the dominant advection in resolving parabolic problems. This scheme offers significant improvements in accuracy and computational efficiency, making it a promising approach to air quality problems. Numerical experiments are developed to validate the enhanced performance of the scheme in comparison to other two-node schemes for dominant advection in both steady and unsteady problems, whether for pure advection problems or those involving both advection and diffusion.

1 Introduction

The planet Earth has undergone and is still undergoing significant transformations, including global climate change caused by the greenhouse effect, as well as pollution of the atmosphere and groundwater. The dispersion of a pollutant and greenhouse gases in the atmosphere, and the reactive transport of a contaminant in groundwater can be modeled by physical principles that describe the distribution of concentration and its evolution over time and space, resulting from advection, diffusion, and reaction processes [12].

Such problem has shown a strong advective dispersion which dominates over diffusion [1]. The advection term represents a challenge that has attracted the interest of several researchers since the 1960s. Traditional first-order schemes are stable and monotonic [3], and tend to be excessively diffusive, leading to inaccurate solutions in solving advection-diffusion-reaction problems. Alternatively, high-order schemes are less dissipative, but can suffer from numerical instabilities that cause non-physical oscillations [5, 10, 11, 15]. Until now, finite-volume advection schemes have continued to be an active area of research, with ongoing efforts to improve accuracy and reduce numerical diffusion and oscillations [4, 16].

Several authors argue that in order to accomplish this goal, one must utilize nonlinear schemes known as High Resolution Schemes (HRS) to circumvent the undesirable nonphysical oscillations presented in HO schemes, or to minimize the diffusivity of stable first-order schemes. These HRS are typically based on flux-correlated transport (FCT) [6, 16], flux limiters that meet the Total Variation Diminishing (TVD) Boundedness criteria, or Normalized Variable Formulation (NVF) that satisfy the Convection Boundedness Criterion (CBC) [8, 9, 17]. HRS nonlinear schemes require at least three nodes and may be computationally demanding and difficult to implement for complicated problems.

In general, the choice of finite-volume scheme depends on the specific problem being solved, as well as the available computational resources and desired accuracy. While finite-volume schemes have many strengths, they can also suffer from limitations such as numerical diffusion, oscillations, and the computational resources and times required.

This paper aims at presenting a scheme for approximating the advection term using only two nodes in a vertex-centered mesh. Through our analysis, we demonstrate the superior performance, efficiency, and simplicity of this scheme for the dominant advection problem compared to other two-node schemes.

This paper is organized as next; In the next Section, we introduce the advection diffusion reaction problem and the discretization steps involved in its resolution using a finite-volume method. Moving on to Section 3, we give an overview of some existing two-node schemes used

to approximate the advection term. Section 4 presents our proposed scheme and explains its implementation. In Section 5, we conclude our work by presenting numerical results and experiments that illustrate the performance of the new scheme in comparison to other two-node schemes for dominant advection in both steady and unsteady problems, whether for pure advection problems or those involving both advection and diffusion. Section 6 presents a summary and outlines potential directions for future work.

2 Problem Formulation

To simplify the calculations and without loss of generality, we will assume that the computational domain is two-dimensional. In the current section, we will outline the mathematical model for pollutant transport in the atmosphere, along with the description of the finite-volume method and construction of numerical fluxes.

2.1 Model Description

Pollutants transport is mathematically described by several models. In this work, we will focus on the unsteady advection-diffusion-reaction model, where every factor plays a role in the particular species dispersion.

We will consider the study domain Ω as a bounded domain in $\mathbb{R}^2$ with a Lipschitzian boundary $\partial\Omega$. Let $[0,T]$ be the time interval with T being a positive real number. At position $x = (x_1, x_2) \in \Omega$ and time $t \in [0,T]$, the advection-diffusion-reaction equation is described as follows:

$$\frac{\partial c(x,t)}{\partial t} - \underbrace{\operatorname{div}\left[K(x,t)\nabla c(x,t)\right]}_{\text{Diffusion}} + \underbrace{\operatorname{div}\left[c(x,t)V(x,t)\right]}_{\text{Advection}} + \underbrace{rc(x,t)}_{\text{Reaction}} = \underbrace{f(x,t)}_{\text{Emissions - Losses}}, \tag{2.1}$$

where c is the species concentration, V is the wind velocity vector, K is the diffusion coefficient, r is the reaction coefficient, and f is the difference between the quantity of the species released by different sources and losses by the species deposition (dry and/or wet) [13].

By adding the initial condition and the boundary conditions to our model, we obtain the following continuous model:

$$\begin{cases} \dfrac{\partial c}{\partial t} - \operatorname{div}(K\nabla c) + \operatorname{div}(cV) + rc = f & \text{in } \Omega \times (0,T) \\ c = g & \text{on } \partial\Omega \times (0,T) \\ c(.,0) = c_0 & \text{in } \Omega, \end{cases} \tag{2.2}$$

where f is a function satisfying $f \in L^2(0,T;L^2(\Omega))$, $g \in L^2(\partial\Omega)$, the scalar r is positive, and $c_0 \in L^2(\Omega)$. Under some assumptions [2, 14] on K, V, r and the initial condition c_0, the problem 2.2 admits a unique solution [18].

The resolution of the system 2.2 will be achieved numerically using the finite-volume method (FVM). In the next section, we introduce the procedure for the temporal and spatial discretization of the problem 2.2.

2.2 Problem Discretization:

We consider a subdivision of the time interval as follows:

$$[0,T] = \cup\left[t_{n-1}, t_n\right], n = 1, \cdots, M_n,$$

such that: $0 = t_0 < t_1 < t_2 < \cdots < t_{M_n-1} < t_{M_n} = T$, and $\Delta t_n = t_n - t_{n-1}$.

There are many approaches to discretize the partial derivative with respect to time, we choose the implicit one:

$$\frac{\partial c(x,t)}{\partial t} = \frac{c^n(x) - c^{n-1}(x)}{\Delta t_n},$$

where $c^n(x) = c(x,t_n)$ and $c^{n-1}(x) = c(x,t_{n-1})$.

To discretize the domain, there are several options available for the finite-volume method, including cell-centered and vertex-centered approaches. For our equation, we opt for a vertex-centered one. To construct a vertex-centered mesh, we start with a given primal finite element triangulation of Ω. Next, we define the dual mesh constructed by control volumes V_i obtained by joining the midpoints of the edges having x_i as extremity with the barycenters of the triangles having x_i as vertex. Let ∂V_i be the boundary of the control volume V_i and γ the edge that separates two control volumes V_i and V_j (see Figure 1).

We note that the unknowns, which are the values of the variables that need to be determined to solve the problem, are associated with the vertices (or nodes) of the triangles within the primal mesh.

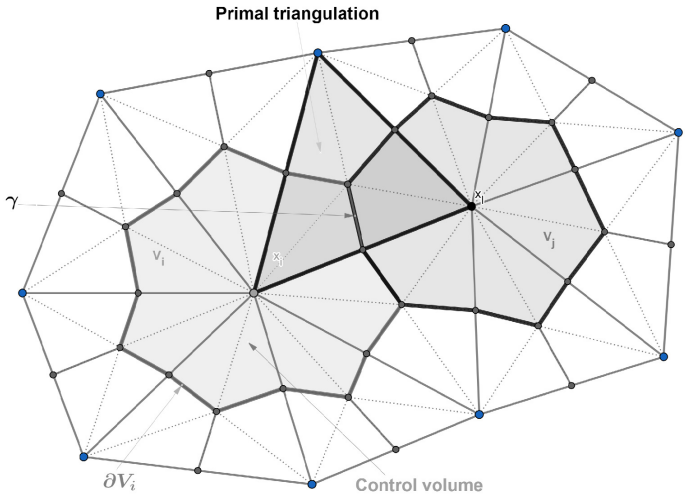

Figure 1: Vertex-Centered Mesh in 2D [14]

Next, we integrate the equation over each control volume V_i, we obtain:

$$\int_{V_i} \frac{c^n - c^{n-1}}{\Delta t_n} dx - \int_{V_i} \operatorname{div}(K \nabla c^n) dx + \int_{V_i} \operatorname{div}(c^n V) dx + \int_{V_i} r c^n dx = \int_{V_i} f^n dx.$$

By applying Green's Formula, we find:

$$\int_{V_i} \frac{c^n - c^{n-1}}{\Delta t_n} dx - \int_{\partial V_i} K \nabla c^n \cdot \mathbf{n}_{\partial V_i} ds + \int_{\partial V_i} c^n V \cdot \mathbf{n}_{\partial V_i} ds + \int_{V_i} r c^n dx = \int_{V_i} f^n dx,$$

where $\mathbf{n}_{\partial V_i}$ is the normal vector outward the boundary ∂V_i. Let $\partial V_i = \cup \gamma$, we have:

$$\int_{V_i} \frac{c^n - c^{n-1}}{\Delta t_n} dx - \sum_{\gamma \subset \partial V_i} \int_{\gamma} K \nabla c^n \cdot \mathbf{n}_{\gamma} ds + \sum_{\gamma \subset \partial V_i} \int_{\gamma} c^n V \cdot \mathbf{n}_{\gamma} ds + \int_{V_i} r c^n dx = \int_{V_i} f^n dx, \tag{2.3}$$

where $\mathbf{n}_{\gamma}$ is the outward unit normal vector of the edge γ.

We note that the numerical flux of diffusion and advection respectively by $\mathscr{F}$ and $\mathscr{G}$ is expressed as next

$$\int_{\gamma} K \nabla c^n \cdot \mathbf{n}_{\gamma} ds \approx |\gamma| \, \mathscr{F}(c_i^n, c_j^n, \mathbf{n}_{\gamma}) \quad \text{and} \quad \int_{\gamma} c^n V \cdot \mathbf{n}_{\gamma} ds \approx |\gamma| \, \mathscr{G}(c_i^n, c_j^n, \mathbf{n}_{\gamma}).$$

Now, the equation (2.3) becomes:

$$|V_i| \frac{c_i^n - c_i^{n-1}}{\Delta t_n} - \sum_{\gamma \subset \partial V_i} |\gamma| \, \mathscr{F}(c_i^n, c_j^n, \mathbf{n}_{\gamma}) + \sum_{\gamma \subset \partial V_i} |\gamma| \, \mathscr{G}(c_i^n, c_j^n, \mathbf{n}_{\gamma}) + |V_i| \, r c_i^n = |V_i| \, f_i^n.$$

Here, $|V_i|$ and $|\gamma|$ are respectively the area of the control volume V_i and the length of the edge γ. Now we explicit the expression of f_i^n, which is an approximation of f^n over the control volume V_i, and we approximate c^n over V_i by c_i^n, with:

$$f_i^n := \frac{1}{|V_i|}\int_{V_i} f^n(x)dx \quad \text{and} \quad c_i^n := \frac{1}{|V_i|}\int_{V_i} c^n(x)dx.$$

For the approximation of the diffusion flux, we approach the normal derivative $\nabla c^n \cdot \mathbf{n}_\gamma$ by:

$$\nabla c^n \cdot \mathbf{n}_\gamma \approx \frac{c_j^n - c_i^n}{d_{ij}},$$

where d_{ij} is the distance between the vertices x_i and x_j.

Therefore, we approach $\int_\gamma K\nabla c^n \cdot \mathbf{n}_\gamma ds$ by:

$$|\gamma|\,\mathscr{F}(c_i^n, c_j^n, \mathbf{n}_\gamma) = K|\gamma|\frac{c_j^n - c_i^n}{d_{ij}}.$$

The remaining tasks are to construct the numerical flux $\mathscr{G}$ to approximate the advection flux and to take into account the boundary condition in the discretization. In the following section, we focus on exploring some existing finite-volume schemes for dominant advection in parabolic equations. We provide an overview of the advantages and disadvantages of the most prominent methods.

3 Approximation of Advection Flux

In order to complete the discretization of the equation using the finite-volume method, we have to present a numerical approximation of the advection flux, $\mathscr{G}(c_i^n, c_j^n, \mathbf{n}_\gamma)$. The main point of this section is to present an overview of the most prominent finite-volume schemes available for dominant advection in parabolic equations.

The approximation of the advection term has been a stimulating area of research for many decades, which enriched the literature with numeros schemes either first-order linear, high-order or high-resolution schemes. In parabolic equations with dominant advection, finite-volume methods may suffer from numerical diffusion and oscillations, adversely affecting the solution's accuracy. Consequently, several techniques have been developed to address these issues.

Most of the linear schemes developed for the advection term are based on a Taylor series development on an one-dimensional cell-centered mesh and are also extended to a two- or three-dimensional cell-centered mesh. We adapt some of famous schemes that are suitable for advection dominant problem, to a vertex-centered 2D mesh:

Central Differencing Scheme (CDS)

This scheme uses a centered approximation to the solution gradient and is second-order accurate. However, it can be susceptible to numerical oscillations in the presence of strong advection. In fact, on an edge γ that separates the control volumes V_i and V_j, we approach c^n by:

$$\frac{c_j^n + c_i^n}{2}.$$

In this context, the numerical approximation of the advection flux is:

$$\mathscr{G}(c_i^n, c_j^n, \mathbf{n}_\gamma) = c_i^n\left(\frac{V\cdot\mathbf{n}_\gamma}{2}\right) + c_j^n\left(\frac{V\cdot\mathbf{n}_\gamma}{2}\right).$$

Upwind Differencing Scheme (UDS)

The numerical approximation of the advection flux in Upwind Differencing Scheme is given by:

$$\mathscr{G}(c_i^n, c_j^n, \mathbf{n}_\gamma) = c_i^n\left(V\cdot\mathbf{n}_\gamma\right)^+ + c_j^n\left(V\cdot\mathbf{n}_\gamma\right)^-,$$

with:

$$(V \cdot \mathbf{n}_\gamma)^+ = \max(V \cdot \mathbf{n}_\gamma, 0) \text{ and } (V \cdot \mathbf{n}_\gamma)^- = \min(V \cdot \mathbf{n}_\gamma, 0).$$

This approach is established according to the sign of the scalar product of the vector V and the outward unit normal vector of V_i on γ. The Upwind Differencing scheme is a first-order accurate method that considers advection by approximating the direction of flow at each cell face. It assumes that the variable being transported moves in the same direction as the flow, which makes it suitable for problems with strong advection. However, this scheme can be overly diffusive and may produce numerical oscillations in some cases.

Hybrid Upwinding Differencing Scheme (HDS)

Hybrid schemes are defined as a combination of both centered and upwind schemes utilizing the Peclet number,

$$Pe_{ij} = \frac{V \cdot \mathbf{n}_\gamma d_{ij}}{K},$$

as a determining factor for the appropriate balance between the two approaches. These schemes aim to incorporate the advantages of both centered and upwind schemes while reducing their limitations.

Here, we present two versions of Hybrid Schemes. The first scheme, (HDS1), is described as next:

$$\mathscr{G}(c_i^n, c_j^n, \mathbf{n}_\gamma) = \begin{cases} c_j^n (V \cdot \mathbf{n}_\gamma) & \text{if} \quad Pe_{ij} < -2, \\ c_i^n (V \cdot \mathbf{n}_\gamma) & \text{if} \quad Pe_{ij} > 2, \\ c_i^n \left(\frac{V \cdot \mathbf{n}_\gamma}{2}\right) + c_j^n \left(\frac{V \cdot \mathbf{n}_\gamma}{2}\right) & \text{otherwise,} \end{cases}$$

while, the second one, (HDS2), is defined by:

$$\mathscr{G}(c_i^n, c_j^n, \mathbf{n}_\gamma) = \begin{cases} c_j^n (V \cdot \mathbf{n}_\gamma) & \text{if} \quad Pe_{ij} < -2 \\ c_i^n (V \cdot \mathbf{n}_\gamma) & \text{if} \quad Pe_{ij} > 2 \\ c_i^n \left(\frac{V \cdot \mathbf{n}_\gamma}{2} + \frac{K}{d_{ij}}\right) + c_j^n \left(\frac{V \cdot \mathbf{n}_\gamma}{2} - \frac{K}{d_{ij}}\right) & \text{otherwise,} \end{cases}$$

The UDS, HDS1 and HDS2 are two nodes Schemes well-suited for large values of Peclet number, especially the two hybrid schemes that combine the advantages of both UDS and CDS. Unfortunately, the truncation error arising from their approximation using the Taylor series is limited to the first order [7, 10, 11, 15]. Therefore, high-order schemes are developed by using at least one additional node.

4 Adaptive Two-Node Finite Volume Scheme

In the current section, we present a new scheme for dominant advection that adaptively addresses the oscillatory and diffusivity concerns. This scheme employs only two nodes to approximate the unknown quantity c on each edge γ separating the control volumes V_i and V_j. We accomplish this by incorporating a corrective term that allows both CDS and UDS approaches to consider the direction of the wind vector and the flow between neighboring volumes. As a result, we can attain stability and good accuracy even in the presence of a high Peclet number.

We present the formulation of the α-adaptive scheme taking into account the sign of the Peclet number and introducing a control parameter α, $\alpha \in [0, 1]$. So, in α-adaptive scheme (α-AS), we approach c_γ by

$$c_\gamma = \begin{cases} \frac{1}{2}(1-\alpha) c_j + \frac{1}{2}(1+\alpha) c_i & \text{if} \quad Pe_{ij} > 0 \\ \frac{1}{2}(1-\alpha) c_i + \frac{1}{2}(1+\alpha) c_j & \text{if} \quad Pe_{ij} < 0. \end{cases} \tag{4.1}$$

Or, generally:

$$c_\gamma = \frac{1}{2}(1 - \epsilon\alpha) c_j + \frac{1}{2}(1 + \epsilon\alpha) c_i,$$

with $\epsilon = \text{sign}(Pe_{ij})$.

This scheme, the α-adaptive scheme, can adaptively address the oscillatory and diffusivity issues through an adaptive parameter α. It can be re-expressed from the decentered form as follows:

$$c_\gamma = c_i + \frac{1}{2}(1 - \epsilon\alpha)(c_j - c_i),$$

and using the centered form, we find this formula:

$$c_\gamma = \frac{c_i + c_j}{2} - \frac{\epsilon\alpha}{2}(c_j - c_i).$$

The therms $(1 - \epsilon\alpha)(c_j - c_i)/2$ and $-\epsilon\alpha(c_j - c_i)/2$ reflect antidispersion and antidiffusion, respectively. The α-adaptive scheme is a generalized form of the two-node schemes, CDS, UDS and HDS, by varying the values of α. Table 1 gives an overview.

Table 1: Values of α for linear schemes

Values of α	**Scheme**
$\alpha = 0$	CDS
$\alpha = 1$	UDS
$\begin{cases} \alpha = 1 & \text{if } \lvert Pe_{ij}\rvert > 2 \\ \alpha = 0 & \text{if } 0 \le \lvert Pe_{ij}\rvert \le 2 \end{cases}$	HUDS1
$\begin{cases} \alpha = 1 & \text{if } \lvert Pe_{ij}\rvert > 2 \\ \alpha = \frac{2}{\lvert Pe_{ij}\rvert} & \text{if } 0 < \lvert Pe_{ij}\rvert \le 2 \end{cases}$	HUDS2

The choice of α is very important, it can be adapted according to the Peclet number. The purpose of this scheme is to reduce the dispersion of the centered approach by incorporating the quantity $-\epsilon\alpha(c_j - c_i)/2$ and to eliminate the inaccurate diffusion caused by the decentered approximation by including the quantity $(1 - \epsilon\alpha)(c_j - c_i)/2$. Furthermore, both quantities are calculated as functions of α. As the stability problem arises with high values of the Peclet number, the choice of α should take into account the presence of high Peclet values, presenting the local characteristics in each mesh element. This ensures that the method reduces oscillations and false diffusion while still maintaining a level of accuracy comparable to that of a second-order scheme.

UDS scheme may introduce excessive artificial diffusion, which leads to a loss of accuracy. Furthermore, the CDS scheme can be susceptible to stability issues and numerical oscillations in the presence of strong advection. To address these limitations of both the UDS and CDS schemes, we use the α-adaptive scheme to balance accuracy and stability by minimizing the value of α to balance the need for accuracy and stability. High-resolution schemes can be computationally expensive, particularly for large-scale or time-dependent problems. In contrast, the α-adaptive scheme is relatively easy to implement and can be applied to a wide range of problems, and ensures that the solution remains physically realistic by correcting the numerical fluxes.

5 Validation and Results

In the current section, to evaluate the performance of the α-AS scheme, a diverse set of test cases is selected. These test cases include problems with known analytical solutions for pure advection problems, and problems involving advection and diffusion, in both steady and unsteady cases. The chosen test cases are commonly used and are represented by the following analytical solutions:

For steady problem:

$$c_1(x, y) = \sin(\pi x)\sin(\pi y),$$

$$c_2(x, y) = (\exp(x) - 1)(\exp(y) - 1),$$

$$c_3(x, y) = 0.1\,(\exp(x) + \exp(y)),$$

$$c_4(x,y) = \frac{(2x-1)(1-y)+1}{9},$$

$$c_5(x,y) = 0.26(x^2+y^2) - 0.48xy,$$

For unsteady problems:

$$c_{1,t}(t,x,y) = \sin(\pi x)\sin(\pi y)\frac{\exp(-t)}{t+1},$$

$$c_{2,t}(t,x,y) = (\exp(x)-1)(\exp(y)-1)\log(t+2),$$

We will evaluate the accuracy of α-AS in comparison to other schemes, CDS, UDS, HDS1 and HDS2, comparing the numerical solution c_h with the analytical solution c, using metrics such as the L^2 norm and L^∞ norm.

In all problems, the required parameters f, c_0, and others are computed in relation to the corresponding exact solution. For each problem, we use discretizations of the domain $\Omega = (0,1)^2$ using a quasi-uniform vertex-centered mesh, and we consider five different meshes with varying maximum step sizes $h_{\max}$. For unsteady problems, we use for numerical simulations a time step $\Delta t_n = 1e-3$.

5.1 First Test: Pure Advection

Here, we consider the following problem of pure advection:

$$\begin{cases} \operatorname{div}(cV) = f & \text{in } \Omega \\ c = g & \text{on } \partial\Omega, \end{cases} \tag{5.1}$$

where f and g are scalar functions, and V is a vector of real numbers.

In Table 2, we compare the accuracy data of the proposed α-adaptive scheme (α-AS) with CDS and UDS, in the pure advection problem. These comparisons revealed the superior performance of the proposed approach with significant improvements in accuracy and computational efficiency, in the framework of two-node approximation schemes.

Table 2: Comparison of error data for pure advection problem 5.1 using CDS, UDS, and α-AS with varying $h_{\max}$ of different quasi-uniform meshes. We used $V = [50, 50]$

		$h_{\max} = 0.116$		$h_{\max} = 0.056$		$h_{\max} = 0.022$	
		L^2 error	L^∞ error	L^2 error	L^∞ error	L^2 error	L^∞ error
c_1	CDS	–	–	–	–	5.80e – 03	2.30e – 02
	UDS	1.54e – 01	3.43e – 01	8.09e – 02	1.17e – 01	3.35e – 02	7.02e – 02
	α-AS	2.16e – 02	6.89e – 02	5.90e – 03	2.55e – 02	9.63e – 04	8.00e – 03
c_2	CDS	–	–	–	–	5.50e – 03	2.44e – 02
	UDS	5.13e – 02	1.44e – 01	2.83e – 02	8.51e – 02	1.26e – 02	4.67e – 02
	α-AS	1.95e – 02	6.14e – 02	3.70e – 03	1.49e – 02	2.64e – 04	1.70e – 03
c_3	CDS	–	–	–	–	1.53e – 04	5.57e – 04
	UDS	4.90e – 03	1.13e – 02	2.70e – 03	6.50e – 03	1.10e – 03	3.30e – 03
	α-AS	3.20e – 04	9.44e – 04	1.88e – 05	8.01e – 05	2.04e – 05	1.51e – 04
c_4	CDS	–	–	–	–	3.00e – 03	1.32e – 02
	UDS	1.84e – 02	3.78e – 02	1.02e – 02	2.27e – 02	4.50e – 03	1.17e – 02
	α-AS	9.80e – 03	2.80e – 02	2.00e – 03	7.50e – 03	2.69e – 04	1.50e – 03
c_5	CDS	–	–	–	–	3.99e – 04	1.70e – 03
	UDS	1.15e – 02	2.62e – 02	6.30e – 03	1.45e – 02	2.70e – 03	6.20e – 03
	α-AS	1.90e – 03	5.90e – 03	4.50e – 04	1.90e – 03	8.02e – 05	5.10e – 04

Figure 2 presents the evolution of the error with respect to the parameter α. Sensitivity investigations are performed to determine the optimal α parameter according to the global configuration for various parameters of the problem, such as the mesh density and the Peclet number. These results provided insight into the scheme's accuracy and versatility, which confirms its suitability for a wide range of applications. The error fluctuates according to the values α, indicating that there exists an optimal value α for each function that results in significantly high accuracy. Typically, our approach yields precise results for various scenarios when α falls within the range of 0.01 to 0.1.

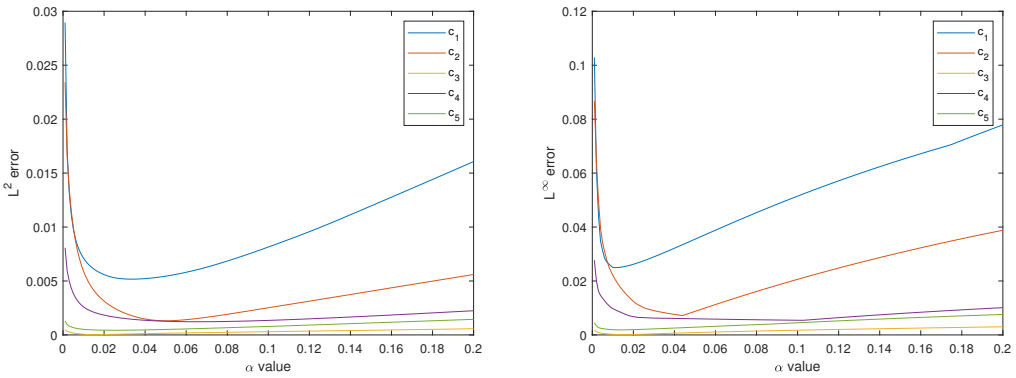

(a) (b)

Figure 2: Plots of errors, L^2 norm (a) and L^∞ norm (b), with respect to the α parameter of the α-adaptive scheme used in numerical resolution of Problem 5.1 for the 5 test functions. Used parameters: $V = [50, 50]$ and $h_{\max} = 0.056$

Now we consider the unsteady version of Problem 5.1:

$$\begin{cases} \dfrac{\partial c}{\partial t} + \operatorname{div}(cV) = f & \text{in } \Omega \times (0,T) \\ c = g & \text{on } \partial\Omega \times (0,T) \\ c(.,0) = c_0 & \text{in } \Omega. \end{cases} \tag{5.2}$$

As shown in Figure 3, the α-adaptive scheme is validated using the selected test cases and performance metrics. The results demonstrated that the α-adaptive scheme accurately and efficiently captured the dominant advection in unsteady problems while enhancing accuracy compared to other schemes. We have selected an α value of $1/60$ for our simulation, which ensures that our scheme performs well over time. Figure 3 shows that α-AS minimizes the accumulation of errors and maintains a good level of accuracy in solving evolutionary problems, compared to other two-node schemes. Additionally, our scheme remains stable even when dealing with coarse meshes and strong wind forces.

5.2 Second Test: Advection and Diffusion

Now, we present a numerical experiment aimed at determining the accuracy of the HDS1, HDS2 and α-AS schemes, for addressing problems involving advection and diffusion. Here, we consider the steady advection-diffusion problem:

$$\begin{cases} -\operatorname{div}(K\nabla c - cV) + rc = f & \text{in } \Omega \\ c = g & \text{on } \partial\Omega. \end{cases} \tag{5.3}$$

Tables 3 and 4 present accuracy data of α-adaptive scheme (α-AS) in comparisons with HDS1 and HDS2, in the problem of advection and diffusion. These comparisons also confirmed the significant improvements in the accuracy of the α adaptive scheme, in the two-node approximation framework, for dominant advection.

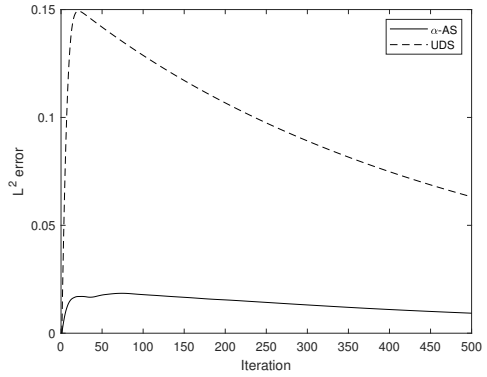

(a) : L^2 error for $c_{1,t}$

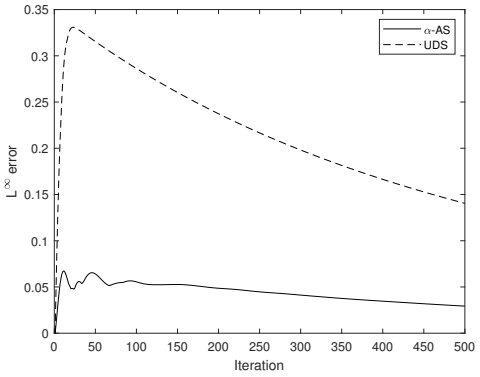

(b) : L^∞ error for $c_{1,t}$

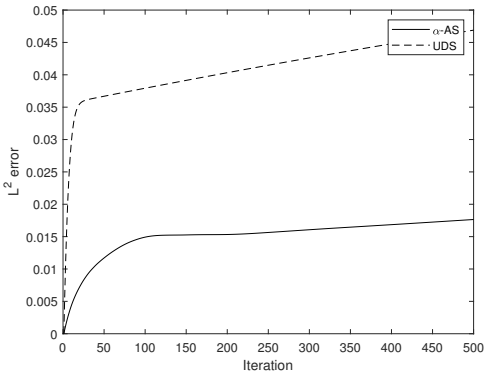

(c) : L^2 error for $c_{2,t}$

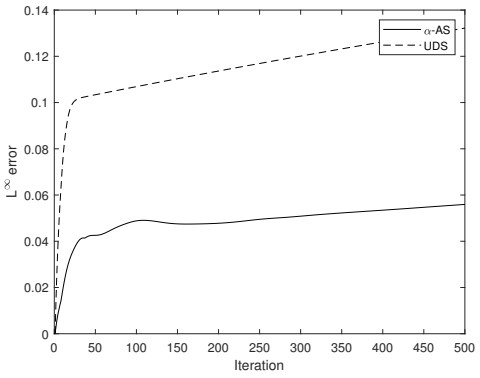

(d) : L^∞ error for $c_{2,t}$

Figure 3: Plots of errors, L^2 and L^∞ norms, with respect to time for UDS and α-AS schemes used in numerical resolution of Problem 5.2 for the 2 test functions $c_{1,t}$ and $c_{2,t}$. Used parameters: $V = [50, 50]$, $h_{\max} = 0.11$ and $\alpha = 1/60$

Figure 4 presents the evolution of the error, L^2 and L^∞, with respect to the parameter α. Sensitivity investigations are performed to determine the optimal α parameter according to the global configuration for various parameters of the problem, such as the mesh density and the Peclet number. These analyses provided insights into the scheme's accuracy and versatility, which confirm its suitability for a wide range of applications.

As seen in the case of pure advection, each function has an optimal value that typically ranges between 0.01 and 0.1 for the diffusion-advection scenario. Selecting the most appropriate value for α can significantly improve the accuracy of solving problems involving advection, diffusion, and reaction processes, especially in cases where advection dominates diffusion.

Now we consider the unsteady version of Problem 5.3:

$$\begin{cases} \dfrac{\partial c}{\partial t} - \operatorname{div}(K\nabla c - cV) + rc = f & \text{in } \Omega \times (0,T) \\ c = g & \text{on } \partial\Omega \times (0,T) \\ c(.,0) = c_0 & \text{in } \Omega. \end{cases} \tag{5.4}$$

In Figure 5, the α-adaptive scheme is validated. The results validated that the α-adaptive scheme accurately and efficiently captured the dominant advection in unsteady problems while enhancing accuracy compared to other schemes. Regarding the unsteady version, Figure 5 indicates that our method maintains good accuracy for error over time, both in the norms L^2 and L^∞. The two hybrid schemes HDS1 and HDS2 exhibit higher error compared to our approach, and they coincide, since both schemes have the same behavior as the UDS scheme for large Peclet values. Furthermore, it is important to mention that α-AS demonstrates excellent performance in

Table 3: Comparison of error data for diffusion-advection Problem 5.3 using HDS1, HDS2, and α-AS with varying $h_{\max}$ of different quasi-uniform meshes. Used parameters: $K = 0.02$, $V = [5, 5]$, $r = 0.1$, $\alpha = 1/60$

		$h_{\max} = 0.116$		$h_{\max} = 0.056$		$h_{\max} = 0.022$	
		L^2 error	L^∞ error	L^2 error	L^∞ error	L^2 error	L^∞ error
c_1	HDS1	1.52e − 01	3.38e − 01	7.99e − 02	1.71e − 01	2.72e − 02	5.35e − 02
	HDS2	1.52e − 01	3.38e − 01	8.00e − 02	1.71e − 01	3.33e − 02	7.15e − 02
	α-AS	1.19e − 02	3.43e − 02	2.77e − 03	1.29e − 02	1.03e − 03	4.52e − 03
c_2	HDS1	5.03e − 02	1.34e − 01	2.78e − 02	8.32e − 02	1.35e − 02	4.81e − 02
	HDS2	5.03e − 02	1.34e − 01	2.77e − 02	8.31e − 02	1.23e − 02	4.58e − 02
	α-AS	4.90e − 03	2.27e − 02	4.49e − 04	3.33e − 03	3.80e − 04	1.11e − 02
c_3	HDS1	4.80e − 03	1.06e − 02	2.60e − 03	6.30e − 03	1.00e − 03	2.90e − 03
	HDS2	4.80e − 03	1.06e − 02	2.60e − 03	6.30e − 02	1.10e − 03	3.20e − 02
	α-AS	1.59e − 04	9.51e − 04	1.12e − 04	8.27e − 04	4.65e − 05	9.25e − 04
c_4	HDS1	1.80e − 02	3.69e − 02	1.00e − 02	2.22e − 02	5.80e − 03	1.47e − 02
	HDS2	1.80e − 02	3.69e − 02	9.90e − 03	2.21e − 02	4.30e − 03	1.11e − 02
	α-AS	3.70e − 03	1.58e − 02	6.53e − 04	4.80e − 03	2.24e − 04	4.10e − 03
c_5	HDS1	1.13e − 02	2.47e − 02	6.10e − 03	1.36e − 02	1.80e − 03	4.00e − 03
	HDS2	1.13e − 02	2.47e − 02	6.20e − 03	1.37e − 02	2.70e − 03	6.00e − 03
	α-AS	7.98e − 04	4.20e − 03	2.56e − 04	1.90e − 03	1.15e − 04	2.00e − 03

Table 4: Comparison of error data for diffusion-advection Problem 5.3 using HDS1, HDS2, and α-AS with different Peclet numbers. Used parameters: $r = 0.1$ and $\alpha = 1/60$

		$Pe_{ij}^{\max} = 8.6$		$Pe_{ij}^{\max} = 57.38$		$Pe_{ij}^{\max} = 4.3\text{e}+03$	
		L^2 error	L^∞ error	L^2 error	L^∞ error	L^2 error	L^∞ error
c_1	HDS1	2.72e − 02	5.36e − 02	3.35e − 02	7.01e − 02	3.35e − 02	7.02e − 02
	HDS2	3.40e − 02	7.16e − 02	3.35e − 02	7.01e − 02	3.35e − 02	7.02e − 02
	α-AS	1.00e − 03	4.50e − 03	7.45e − 04	4.70e − 03	9.63e − 04	8.30e − 03
c_2	HDS1	1.35e − 02	4.81e − 02	1.26e − 02	4.65e − 02	1.26e − 02	4.67e − 02
	HDS2	1.23e − 02	4.58e − 02	1.26e − 02	4.65e − 02	1.26e − 02	4.67e − 02
	α-AS	3.80e − 04	1.11e − 03	1.70e − 04	2.50e − 03	2.36e − 04	1.50e − 03
c_3	HDS1	1.00e − 03	2.90e − 03	1.10e − 03	3.30e − 03	1.20e − 03	3.30e − 03
	HDS2	1.10e − 03	3.20e − 03	1.10e − 03	3.30e − 03	1.20e − 03	3.30e − 03
	α-AS	4.65e − 05	9.25e − 04	3.30e − 05	4.02e − 04	2.56e − 05	1.97e − 04
c_4	HDS1	5.80e − 03	1.47e − 02	4.50e − 03	1.17e − 02	4.50e − 03	1.17e − 02
	HDS2	4.30e − 03	1.11e − 02	4.50e − 03	1.17e − 02	4.50e − 03	1.17e − 02
	α-AS	2.24e − 04	4.10e − 03	2.01e − 04	2.20e − 03	2.55e − 04	1.60e − 03
c_5	HDS1	1.80e − 03	4.00e − 03	2.70e − 03	6.10e − 03	2.70e − 03	6.20e − 03
	HDS2	2.70e − 03	6.00e − 03	2.70e − 03	6.10e − 03	2.70e − 03	6.20e − 03
	α-AS	1.15e − 04	2.00e − 03	8.11e − 05	9.15e − 04	8.53e − 05	5.85e − 04

resolving parabolic problems with dominant Advection. In conclusion, the successful validation of the α-adaptive scheme for dominant advection in elliptic or parabolic equations establishes its potential compared to existing two-node methods.

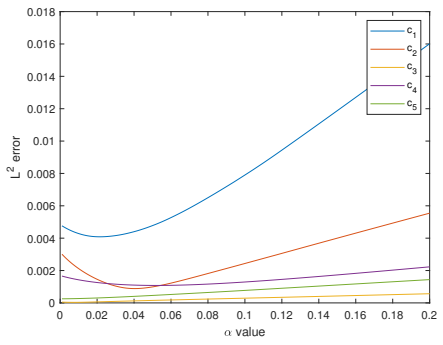

(a)

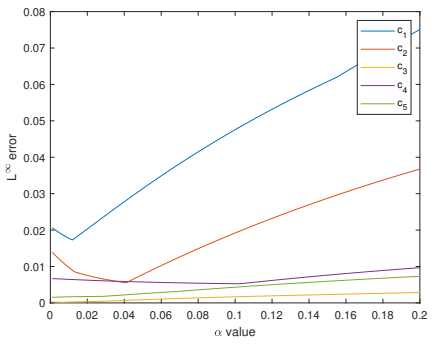

(b)

Figure 4: Plots of errors, L^2 norm (a) and L^∞ norm (b), with respect to the α parameter of the α-adaptive scheme used in numerical resolution of Problem 5.3 for the 5 test functions. Used parameters: $K = 0.003$, $V = [5, 5]$, $h_{\max} = 0.056$, and $r = 0.1$

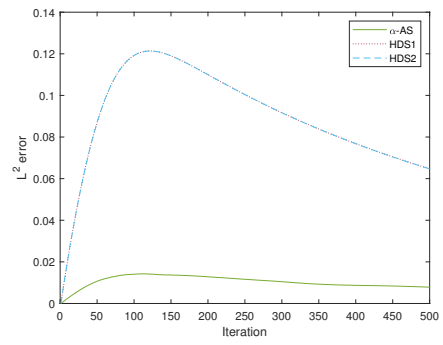

(a) : L^2 error for $c_{1,t}$

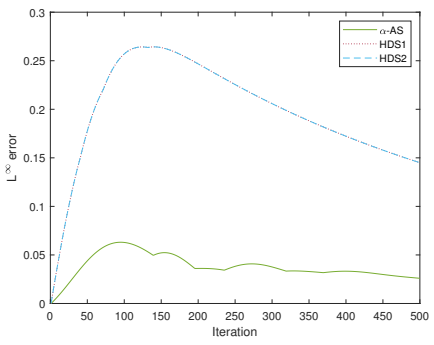

(b) : L^∞ error for $c_{1,t}$

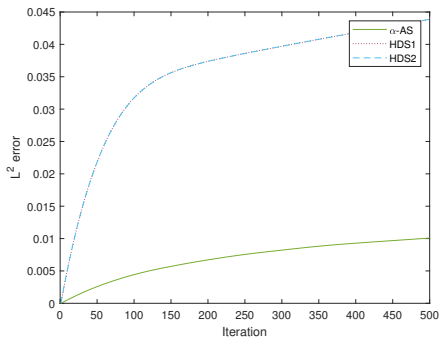

(c) : L^2 error for $c_{2,t}$

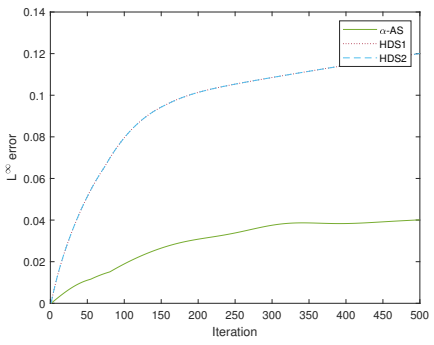

(d) : L^∞ error for $c_{2,t}$

Figure 5: Plots of errors, L^2 and L^∞, with respect to time for HDS1, HDS2, and α-AS schemes used in numerical resolution of Problem 5.4 for the 2 test functions $c_{1,t}$ and $c_{2,t}$. $K = 0.02$, $V = [5, 5]$, $r = 1$, $h_{\max} = 0.11$, and $\alpha = 1/60$

6 Conclusion

The proposed α-adaptive scheme has demonstrated excellent performance and efficiency in approximating the advection term, for steady or unsteady problems, and remains effective regardless of the existence or absence of diffusion. This scheme has proven to be stable and accurate, particularly in cases where advection dominates and the Peclet number is large. Compared to

other two-node schemes, the α-scheme consistently performs well, demonstrating its robustness and reliability. Furthermore, this scheme is easy to implement, requires minimal resources and computation time, and can easily be adapted to higher Peclet numbers.

The choice of values α plays a crucial role in determining the effectiveness of the scheme. Specifically, if α is set to 0, the resulting scheme coincides with the CDS scheme, which is known to be unstable due to virtual oscillations. On the other hand, if α is set to 1, the scheme becomes the UDS scheme, which has limited accuracy. Therefore, to obtain more accurate solutions, we have opted to investigate the optimal α value. By making this choice, it becomes possible to ensure that the solution remains stable and accurate, even with a high Peclet number. In conclusion, the successful validation of the α-adaptive scheme for dominant advection in elliptic or parabolic equations establishes its potential to address real-world problems, offering enhanced performance and versatility compared to existing two-node methods.

Moving forward, there are numerous potential paths for future investigations about the α-adaptive scheme. A possible direction to develop an algorithm to find the optimal value for α according to the local configuration for various parameters of the problem, such as the mesh density and local Peclet values. Another possible direction could be to create a generalized scheme by considering the local configuration. This can be done by introducing a real-valued function α, which depends on the Peclet number.

References

[1] H. Ahmadi, M. M. Namin, and F. Kilanehei. Development a numerical model of flow and contaminant transport in layered soils. *Adv. Environ. Res.*, **5(4)**, 263–282 (2016).

[2] B. Amaziane, A. Bergam, M. El Ossmani, and Z. Mghazli. A posteriori estimators for vertex centred finite volume discretization of a convection–diffusion-reaction equation arising in flow in porous media, *Int. J. Numer. Methods Fluids*, **59(3)**, 259–284 (2009).

[3] V. G. Ferreira, R. A. B. De Queiroz, G. A. B. D. Lima, R. G. Cuenca, C. M. Oishi, J. L. F. D. Azevedo, and S. McKee. A bounded upwinding scheme for computing convection-dominated transport problems. *Comput. Fluids*, **57**, 208–224 (2012).

[4] J. H. Ferziger, M. Perić, and R. L. Street. Computational methods for fluid dynamics, **4**, *Springer*, (2002).

[5] A. Kaushik. Critical evaluation of four differencing schemes for a steady convection-diffusion problem. *Res. j. math. stat. sci.*, **2320**, 6047 (2016).

[6] D. Kuzmin, R. Löhner, and S. Turek. Flux-corrected transport: principles, algorithms, and applications. *Springer Science & Business Media*, (2012).

[7] P. Majumdar. Computational methods for heat and mass transfer. *Taylor & Francis*, (2005).

[8] D. McBride. Vertex-based discretisation methods for thermo-fluid flow in a finite volume-unstructured mesh context. *Ph. D. thesis, University of Greenwich*, (2003).

[9] F. Moukalled, L. Mangani, and M. Darwish. The finite volume method. *Springer International Publishing*, (2016).

[10] S. E. Norris. A parallel navier stokes solver for natural convection and free surface flow. *Ph. D. thesis, School of Aerospace, Mechanical and Mechatronic Engineering, University of Sydney, Australia*, (2000).

[11] S. V. Patankar. Numerical heat transfer and fluid flow. *CRC press*, (2018).

[12] C. E. A. Rodriguez and J. F. Velazquez. Cfd simulation of heat and mass transfer for climate control in greenhouses. *In Heat and Mass Transfer-Advances in Science and Technology Applications*. IntechOpen, (2019).

[13] F. Souley. Simulation numérique du transport spatial et temporel des concentrations de CO2 et de CH4 atmosphériques et comparaisons avec les observations. *Ph. D. thesis, Université Laval*, (2010).

[14] H. Tayeq, A. Bergam, A. El Harrak, and K. Khomsi. Self-adaptive algorithm based on a posteriori analysis of the error applied to air quality forecasting using the finite volume method. *Discrete Contin. Dyn. Syst. - S*, **14(7)**, 2557– 2570 (2021).

[15] H. K. Versteeg and W. Malalasekera. An introduction to computational fluid dynamics: the finite volume method. *Pearson education*, (2007).

[16] Y. Wang and K. Hutter. Comparisons of numerical methods with respect to convectively dominated problems. *Int. J. Numer. Methods Fluids*, **37(6)**, 721–745 (2001).

[17] N. P Waterson and Herman Deconinck. Design principles for bounded higher-order convection schemes–a unified approach. *J. Comput. Phys.*, **224(1)**, 182–207 (2007).

[18] R. Dautray and J. -L. Lions. Mathematical Analysis and Numerical Methods for Science and Technology. *Springer-Verlag, Berlin*, (1992).

Author information

Abdelaziz Chahed, SMAD, FPL, Abdelmalek Essaadi University, Tetouan, Morocco.
E-mail: abdelaziz.chahed@etu.uae.ac.ma

Amal Bergam, SMAD, FPL, Abdelmalek Essaadi University, Tetouan, Morocco.
E-mail: abergam@uae.ac.ma

Anouar El Harrak, MMA, FPL, Abdelmalek Essaadi University, Tetouan, Morocco.
E-mail: anouarelharrak1@gmail.com

Hatim Tayeq, SMAD, FPL, Abdelmalek Essaadi University, Tetouan, Morocco.
E-mail: tayeq.hatim@gmail.com